Multi-service Signal Multiplexing and Isolation for Physical-Layer Network Slicing (PNS)

Lei Zhang, Ayesha Ijaz, Juquan Mao, Pei Xiao and Rahim Tafazolli

5G Innovation Centre (5GIC), Institute for Communication Systems (ICS)

University of Surrey

Guildford, GU2 7XH, UK

Email: {lei.zhang, a.ijaz, juquan.mao, p.xiao, r.tafazolli}@surrey.ac.uk

Abstract—Network slicing has been identified as one of the most important features for 5G and beyond to enable operators to utilize networks on an as-a-service basis and meet the wide range of use cases. In physical layer, the frequency and time resources are split into slices to cater for the services with individual optimal designs, resulting in services/slices having different baseband numerologies (e.g., subcarrier spacing) and / or radio frequency (RF) front-end configurations. In such a system, the multi-service signal multiplexing and isolation among the service/slices are critical for the Physical-Layer Network Slicing (PNS) since orthogonality is destroyed and significant inter-service/ slice-band-interference (ISBI) may be generated. In this paper, we first categorize four PNS cases according to the baseband and RF configurations among the slices. The system model is established by considering a low out of band emission (OoBE) waveform operating in the service/slice frequency band to mitigate the ISBI. The desired signal and interference for the two slices are derived. Consequently, one-tap channel equalization algorithms are proposed based on the derived model. The developed system models establish a framework for further interference analysis, ISBI cancelation algorithms, system design and parameter selection (e.g., guard band), to enable spectrum efficient network slicing.

Index Terms—Network slicing, physical layer network slicing (PNS), inter-service / slice-band-interference (ISBI), isolation and multiplexing, waveform, multi-service

I. INTRODUCTION

The next generation wireless communication (5G) and beyond will enable a fully mobile and connected society, which requires to support a variety of very diverse and extreme requirements in terms of latency, throughput, capacity, and availability. Network slicing offers an effective way to meet the requirements of all use cases and enables design, deployment, customization, and optimization of different network slices on *a common infrastructure* [1], [2], [3]. However, due to the extreme diverse requirement among the services and use cases, the service configurations in different resource slices may be significantly different [4], [5]. From the physical layer perspective, the differences could be either in baseband (BB) (e.g., frame structure, subcarrier spacing, etc) or / and in radio frequency (RF) front-end (e.g., processing bandwidth). For example, the massive machine type communications (mMTC), identified as one of the main scenarios for 5G, might require smaller subcarrier spacing and larger symbol duration to support massive delay-tolerant devices. On the other hand, vehicle to vehicle (V2V) communications have much more

stringent latency requirements, which necessitate significantly small symbol duration compared with the mMTC scenario. Due to the huge discrepancy in this design criteria and specifications, it is cumbersome to design a unified all-in-one radio frame structure to meet all requirements for all types of services. In addition, low-end MTC devices might have limited hardware complexity and signal processing capabilities, the RF bandwidth especially the analog to digital (A/D, or D/A for uplink) converter might be significantly smaller than the full system bandwidth as compared to the normal UE or base station.

The multiple services can be multiplexed in one system in orthogonal frequency or time slices. Compared with the time domain multiplexing (TDM), frequency division multiplexing (FDM) has several advantages such as good forward compatibility, ease of supporting services with different latency requirements, energy saving by turning off some transmit time intervals (TTIs) etc [6]. However, combining multiple services/slices with different BB and RF configurations into one baseband is also more challenging than TDM due to the loss of orthogonality, resulting in inter-service-band-interference (ISBI) [5].

How to multiplex and isolate the signals to minimize the interference and overhead among the slices/services is one of the main challenges to enable spectrum efficient network slicing. In principle, the overall interference level depends on the subcarrier spacing and RF bandwidth differences among the slices and the GB between the service bands. Moreover, the choice of waveform is also a key factor to determine the interference level. Therefore, a framework model by taking the BB and RF differences and low out of band emission (OoBE) waveform into account is a foundation for the PNS design in terms of parameter selection, algorithm design, frame structure design, etc.

To analyze the performance loss caused by services' BB imparity, [5] has proposed a comprehensive framework on a multi-service system to support multiple types of services/slices each having different subcarrier spacing and frame structure. The system modeling and performance analysis in terms of ISBI have been given, with a proposed precoding algorithm to cancel the ISBI at the BS for downlink transmission. In addition, as an exemplary case of resource slices using different RF configurations, In-band and Guard-

band Narrow-band Internet of Things (NB-IoT) utilizing the resource blocks within a normal or guard-band Long Term Evolution (LTE) carriers, have been adopted in LTE-Advanced Pro as an important feature, where the NB-IoT devices using as narrow bandwidth as 180 kHz are multiplexed with the LTE UEs and share the same infrastructure (e.g., BS) [7]. The coexistence of LTE and IoT signals has been investigated by 3GPP via extensive simulations [7]. Other studies on NB-IoT focus on either frame structure design [8], random access networks [9] or scheduling [10]. In addition, the NB-IoT is based on orthogonal frequency division multiplexing (OFDM) to make the system compatible to the legacy LTE UEs. In such case, the interference may be significantly large when multiple chunks of RBs are used to support massive IoT devices. Therefore, a new system model considering low OoBE waveforms is necessary to analyse the impact caused by the RF processing imparity among the service bands. In addition, the models can provide a basic framework for 5G BB frame structure and RF bandwidth selection.

In this paper, we will first build a multi-service system framework for physical layer network slicing and categorize the four possible cases by considering the differences in both BB and RF configurations, with a subband filtered multicarrier (SFMC) waveform operated on the top of slice signals to reduce the ISBI. By considering the most general case, i.e, the two slices with different BB subcarrier spacing and RF processing bandwidth, the downlink system model for PNS is established. Note that the work can be extended to the uplink transmission straightforwardly. Based on the established system model, one-tap channel equalization algorithms and expressions for ISBI due to the joint RF band BB configurations mismatches are derived.

Notations: $\{\cdot\}^H$ and $\{\cdot\}^T$ stand for the Hermitian conjugate and transpose operation, respectively. We use $\mathbb{E}\{\mathbf{A}\}$ and diag$\{\mathbf{A}\}$ to denote the expectation of matrix $\mathbf{A}$ and a diagonal matrix formed by taking the diagonal elements of $\mathbf{A}$, respectively. However, diag$\{\mathbf{a}\}$ denotes forming a diagonal matrix $\mathbf{A}$ using the vector $\mathbf{a}$. $\mathbf{I}_{M \times M}$ and $\mathbf{0}_{M \times N}$ refer to M dimension identity matrix and an $M \times N$ zero matrix, respectively.

II. FOUR CASES OF PHYSICAL-LAYER NETWORK SLICING (PNS)

Without loss of generality, in this paper we will only consider two physical layer slices that may have different configurations for the two use cases. We assume the two access resource slices are adjacent to each other with or without a guard-band between them to mitigate the ISBI. Note that each access slice in PHY may be assigned to multiple users that have the same configuration. However, different slices may have different optimal BB and / or RF configurations. In addition, different types of users with similar communication requirements (e.g., data rate, complexity, etc.) may be categorized into the same resource slice. To simplify our derivations and without loss of generality, we assume that each slice contains one UE only. In physical layer, the

following four cases encompass the differences among all of the UE, application, and service: the two slices have the same BB and same RF (SBSR), the two slices have different BB and same RF (DBSR), the two slices have the same BB and different RF (SBDR), the two slices have different BB and different RF (DBDR).

Case 1 - SBSR: the RF and BB in the two access resource slices use the same configurations. In addition, the RF processing bandwidth in the two UEs are equal or larger than the whole system bandwidth. As a result, the two slices can be orthogonally multiplexed without generating any interference by using the classic OFDM waveform only. Note that LTE/LTE-A is such a kind of system wherein all UEs and services have the same configuration.

Case 2 - DBSR: The two UES allocated in the two access resource slices have the same RF processing bandwidth. However, the baseband numerologies utilized in the two slices are different. For example, one UE is a MTC device and other one is a legacy LTE UE. To support massive MTC and enable sufficient power boosting, the subcarrier spacing in MTC should be smaller than the legacy user, resulting in different frame structures. The system model and interference analysis have been discussed in [5] thoroughly.

Case 3 - DBSR: Unlike Case two, Case three assumes the two UEs that occupy the two slices have different RF configurations (at least on is smaller than the system bandwidth to save cost and complexity), but with the same BB numerology. An example of such a scenario is the narrowband internet of things (NB-IoT), where the processing bandwidth in IoT UE is only 180 kHz, i.e. much smaller than the BS and legacy LTE UEs (e.g., 20 MHz). Due to the sampling rate mismatch between the transmitted and received signals, system orthogonality will be destroyed and may invalidate the widely-used signal detection algorithms (e.g., channel equalization/estimation) [11].

Case 4 - DBDR: Case four considers both RF and BB imparity among the access slices. In this case, the ISBI will be generated from two sources. This is the most complex Case that may have the worst performance in terms of ISBI. However, this case probably is the most practical one, since it can maximize the potential of the network slicing to cater for the individual service requirements by optimizing both RF and BB configurations. In addition, it is also the most generic case in terms of theoretical analysis. For these reasons, we will build system model and analyze the interference based on this case.

The interference level in Case 2, 3 and 4 can be either reduced by inserting guard-band between the two service bands, resulting in spectrum efficiency reduction, or by using subband filtering to mitigate the interference. In this paper, we will consider low OoBE SFMC waveform operating on the top of each resource slice to reduce interference.

III. DBDR PNS SYSTEM MODEL

Suppose the system bandwidth B is normalized, i.e., $B = 1$ and the slices 1 and 2 have the bandwidth B_1 and B_2,

respectively, with a guard band ΔB_1 in between. Let us define ΔB_0 and ΔB_2 as other used or unused bandwidth/slices on the left and right of slices 1 and 2, respectively. M_1 and M_2 are the number of subcarriers in the first and second slices. Therefore, the discrete Fourier transform (DFT) sizes (or base band sampling rate) for the two slices are:

$$N_i = \frac{M_i}{B_i}, \quad \text{for} \quad i = 1, 2 \qquad (1)$$

Note that the bandwidth B_i and number of subcarriers M_i selection will make sure that N_i is a positive integer.

1) Baseband numerology imparity: In principle, different slices/services can use arbitrary symbol duration and subcarrier spacing in its frequency bands. However, it is beneficial to design a PNS system with an integral least common multiplier (LCM) symbol duration T_{LCM} for all services, e.g., slices 1 and 2 symbol durations satisfy the relationship $\Delta T_2 = 2\Delta T_1$ (which implies that subcarrier spacing $\Delta f_1 = 2\Delta f_2$). In fact, this design principle has been adopted as a basis for the current 5G air interface standardization. For example, assuming the subcarrier spacing for eMBB is 15 kHz, the subcarrier spacing for mMTC should be, e.g., 15/8, 15/4, 15/2 kHz, etc. Therefore, we assume that the subcarrier spacing in slice 1 is G times wider than the one in slice 2 i.e.

$$\Delta f_1 = G\Delta f_2 \qquad (2)$$

where $G \in \mathbb{Z} > 1$.

2) RF imparity: Similar to the BB case, the RF processing bandwidth of the two UEs may be integral multiples of each other to facilitate DFT (or inverse DFT (IDFT)) processing and RF design. In principle, the RF processing bandwidth difference in the two slices may not be correlated with the BB imparity. However, a particularly interesting and practical use case is the mMTC, whose subcarrier spacing and RF processing bandwidth are smaller than the eMBB case. Therefore, in the next, we will consider that the sampling rate of slice 1 and slice 2 has the following relationship

$$S_1 = QS_2 \qquad (3)$$

where $Q \in \mathbb{Z} > 1$.

3) Subband filtering waveforms: Many waveforms have been proposed for 5G to reduce the out of band emission, such as subcarrier filtered multicarrier system including filterbank multi-carrier (FBMC) [12], [13], [14] and generalized frequency division multiplexing (GFDM) [15], [16], subband filtered multicarrier (SFMC) system including universal filtered multi-carrier (UFMC) [17], [5], [18], [19] and filtered orthogonal frequency division multiplexing (F-OFDM) [20], [21], [22]. Amongst them, SFMC system is a promising candidate due to its excellent tradeoff between performance and complexity. In this paper, we will consider F-OFDM as an example. However, the results are extendable to all other waveforms. Let us denote the subband filter impulse response for the two resource slices as

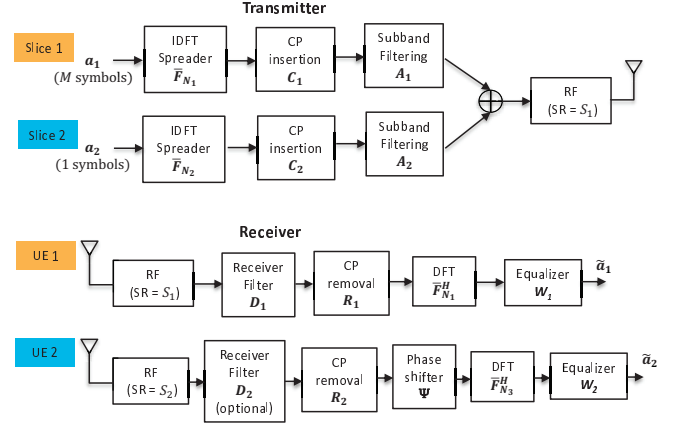$$\mathbf{g}_1 = [g_1(1), g_1(2), \cdots, g_1(L_{F,1})]^T \qquad (4)$$

Fig. 1. Transmitter and receiver block diagram of DBDR physical layer network slicing.

$$\mathbf{g}_2 = [g_2(1), g_2(2), \cdots, g_2(L_{F,2})]^T \qquad (5)$$

where $L_{F,1}$ and $L_{F,2}$ are the filter length.

Thus, the frequency domain filter response can be obtained by the Fourier transform as:

$$\mathbf{f}_1 = \mathbf{F}_{N_1}^H \tilde{\mathbf{g}}_1 \qquad (6)$$

$$\mathbf{f}_2 = \mathbf{F}_{N_2}^H \tilde{\mathbf{g}}_2 \qquad (7)$$

where $\mathbf{F}_{N_1}^H$ and $\mathbf{F}_{N_2}^H$ are power normalized DFT matrices with dimension N_1 and N_2, respectively. $\tilde{\mathbf{g}}_1$ and $\tilde{\mathbf{g}}_2$ are the zero padded versions of $\mathbf{g}_1$ and $\mathbf{g}_2$ with length N_1 and N_2, respectively.

Note that the the matched filter can be applied at the receiver of UE 1 to reject the interference from the adjacent subband/slice. However, baseband filtering will not work in the UE 2 since the signals will be down sampled by a factor of Q in the A/D converter. However, the RF filter will take the role of mitigating the interference from resource slice 1.

4) Transmitter Processing: The signal in the i-th service/slice after the IDFT and CP insertion can be written in matrix form as:

$$\mathbf{b}_i = \mathbf{C}_i \tilde{\mathbf{F}}_{N_i} \mathbf{a}_i , \qquad (8)$$

where $\mathbf{C}_i = [\mathbf{0}_{L_{CP,i} \times (N_i - L_{CP,i})}, \mathbf{I}_{L_{CP,i}}; \mathbf{I}_{N_i}] \in \mathbb{R}^{L_i \times N_i}$ with $L_{CP,i}$ being the CP length for the i-th service/slice and $L_i = N_i + L_{CP,i}$ is the symbol duration of the i-th service/slice in samples. $\tilde{\mathbf{F}}_{N_i} \in \mathbb{C}^{N_i \times M_i}$ is a submatrix of the N_i-point normalized and *frequency shifted* IDFT matrix. The element in the l-th row and n-th column of $\tilde{\mathbf{F}}_{N_i}$ is $d_{l,n} = \frac{1}{\sqrt{N_k}} e^{j \cdot 2\pi l(n + \eta_i)/N_i}$, where η_i is the frequency shift given as

$$\eta_i = N_i \left(\sum_{m=1}^{i-1} B_m + \sum_{m=0}^{i-1} \Delta B_m \right). \qquad (9)$$

With the waveform subband filtering, we can write the output of the subband filter for the i-th slice as

$$\mathbf{c}_i = \mathbf{A}_i \mathbf{b}_i , \qquad (10)$$

where $\mathbf{A}_i \in \mathbb{C}^{(L_i+L_{F,i}-1)\times L_i}$ is a matrix form of subband filtering operation. It is a Toeplitz matrix with its first column and first row being $[\mathbf{g}_i; \mathbf{0}_{(L_{F,i}-1)\times 1}]$ and $[g_i(0), \mathbf{0}_{1\times(L_i-1)}]$, respectively.

According to equation (2), the symbol duration of the slice $\mathbf{c}_2$ is G times longer than $\mathbf{c}_1$. Let us denote $\mathbf{c}_1(k)$ as the k-th symbol of slice 1, then $\bar{\mathbf{c}}_1$ is a vector formed from the contiguous G symbols in the slice i.e. $\bar{\mathbf{c}}_1 = [\mathbf{c}_1(1); \mathbf{c}_1(2); \cdots; \mathbf{c}_1(G)]$. The signal in one LCM symbol before transmission over the channel can be written as:

$$\mathbf{p} = \bar{\mathbf{c}}_1 + \mathbf{c}_2 \qquad (11)$$

5) Receiver Processing: Let us assume the channel between the transmitter and the i-th user is $\mathbf{h}_i = [h_i(1), h_i(2), \cdots, h_i(L_{CH,i})]$ where $L_{CH,i}$ is the length of the channel in samples. Using equation (11), the received signal at the i-th user can be written as $\mathbf{y}_i = \mathbf{h}_i * \mathbf{p} + \mathbf{w}_i$, where $\mathbf{w}_i$ is the noise vector with each element having a distribution $w_i(l) \sim \mathcal{CN}(0, \sigma_i^2)$.

At the receiver, due to the different RF and base band configurations, the two UEs processing also varies. For the first UE with smaller symbol duration and same RF bandwidth with BS, the received signal will be split into G symbols and follows the OFDM processing directly. Specifically, for UE 1, $\mathbf{y}_1$ is split into G non-overlapping symbols each being a length L_1 vector for receiver baseband processing. Let us define $\mathbf{p}_k$ and $\mathbf{w}_{1,k}$ as the $[(k-1)L_1+1]$-th to kL_1-th element of $\mathbf{p}$ and $\mathbf{w}_1$, respectively. Then the signal (before channel equalization) of the k-th symbol of the first UE can be written as

$$\mathbf{y}_{1,k} = \tilde{\mathbf{F}}_{N_1}^H \mathbf{R}_1 \mathbf{A}_1^H \mathbf{B}_1 (\mathbf{p}_k + \mathbf{w}_{1,k}), \text{for} \quad k = 1, \cdots, G \quad (12)$$

where $\mathbf{R}_1$ and $\mathbf{A}_1^H$ are the CP removal and matched matrices with correct dimension, respectively. $\mathbf{B}_1$ is the Toeplitz channel matrix with its first column and row being $[\mathbf{h}_1, \mathbf{0}_{(L_1-L_{CH,1}-1)\times 1}]^T$ and $[h_1(1), \mathbf{0}_{1\times L_1-1}]$, respectively. Note that the inter-symbol-interference (ISI) is not considered in the system model since it could be neglected as compared to the ISBI when the waveform is well designed. However, the analytical ISI expression can be found in [5].

For the second UE assigned within the second slice, the length of $\mathbf{p}$ is the same as one symbol in slice two. However, due to lower RF processing bandwidth, the signal will be down-sampled by a factor of Q, phase shifted, and the normal N_2-point OFDM processing performed. The signal of the second UE (before channel equalization) can be written as:

$$\mathbf{y}_2 = \tilde{\mathbf{F}}_{N_2}^H \mathbf{R}_2 \mathbf{\Psi} \mathbf{D}_G \mathbf{Z}_2^H \mathbf{B}_2 (\mathbf{p} + \mathbf{w}_2), \qquad (13)$$

where $\mathbf{D}_G$ is the down-sampling matrix by a factor of Q. $\mathbf{\Psi}$ is a diagonal matrix phase shift due to the RF processing bandwidth mismatch. The i-th diagonal element of $\mathbf{\Psi}$ is $e^{-j2\pi i \eta_2/M_2}$. $\mathbf{R}_2$ is the CP removal matrix with correct dimension. Note that due to down sampling at UE 2, the baseband subband filtering can not work well to reject the interference from other slices. Instead, the RF filter takes this role. Here we assume $\mathbf{Z}_2^H$ is a baseband filter matrix that has

the same response as the RF filter, i.e., using baseband filter $\mathbf{Z}_2^H$ on the received digital signal is equivalent to performing RF filtering on the analog signal.

6) One-tap Channel Equalization: For the first UE, by using (8), (10) and (11), we can rewrite equation (12) as:

$$\begin{aligned}\mathbf{y}_{1,k} &= \tilde{\mathbf{F}}_{N_1}^H \mathbf{R}_1 \mathbf{A}_1^H \mathbf{B}_1 [\mathbf{A}_1 \mathbf{C}_1 \tilde{\mathbf{F}}_{N_1} \mathbf{a}_1(k) \\ &+ \bar{\mathbf{A}}_{2,k} \mathbf{C}_2 \tilde{\mathbf{F}}_{N_2} \mathbf{a}_2 + \mathbf{w}_{1,k}]\end{aligned} \qquad (14)$$

where $\bar{\mathbf{A}}_{2,k}$ is a sub-matrix of $\mathbf{A}_{2,k}$ taking its $(kL_1 + 1)$-th to $(k+1)L_1$-th rows. With sufficient CP length and without considering the ISI, we have $\mathbf{R}_1 \mathbf{A}_1^H \mathbf{B}_1 \mathbf{A}_1 \mathbf{C}_1 = \mathbf{A}_{1,cir}^H \mathbf{B}_{1,cir} \mathbf{A}_{1,cir}$, where $\mathbf{A}_{1,cir}^H$, $\mathbf{B}_{1,cir}$ and $\mathbf{A}_{1,cir}$ are circular matrices. Using the circular convolution property between the first slice's signal in the k-th symbol, we can write (14) as:

$$\mathbf{y}_{1,k} = \mathbf{H}_{eff,1} \mathbf{a}_1(k) + \mathbf{e}_{1,k} + \mathbf{v}_{1,k} \qquad (15)$$

where $\mathbf{H}_{eff,1} = \mathbf{H}_1 \mathbf{F}_1 \mathbf{F}_1^H$ is the effective channel taking the filter responses into consideration. $\mathbf{e}_{1,k} = \tilde{\mathbf{F}}_{N_1}^H \mathbf{R}_1 \mathbf{A}_1^H \mathbf{B}_1 \bar{\mathbf{A}}_{2,k} \mathbf{C}_2 \tilde{\mathbf{F}}_{N_2} \mathbf{a}_2$ and $\mathbf{v}_{1,k} = \tilde{\mathbf{F}}_{N_1}^H \mathbf{R}_1 \mathbf{A}_1^H \mathbf{B}_1 \mathbf{w}_{1,k}$ is interference from the second slice and noise after DFT operation, respectively. Note that the interference $\mathbf{e}_{1,k}$ at different symbols in one LCM duration (i.e., k takes different values) might be different since the symbols in slice 1 overlap with different parts of slice 2.

The first term $\mathbf{H}_{eff,1} \mathbf{a}_1(k)$ is the desired signal and it can be seen that the signal has been written as a point-wise multiplication with the filter and channel frequency response. Thus, one-tap channel equalization can be performed.

For the second UE, by using (8), (10) and (11) and similar to the UE 1, we can rewrite equation (13) as:

$$\mathbf{y}_2 = \mathbf{H}_{eff,2} \mathbf{a}_2 + \mathbf{e}_2 + \mathbf{v}_2 \qquad (16)$$

where $\mathbf{H}_{eff,2} = \mathbf{H}_2 \mathbf{F}_2 \mathbf{\Upsilon}_2^H$ is the effective channel of UE 2 with $\mathbf{\Upsilon}_2^H$ being the RF filter frequency response in UE 2. $\mathbf{e}_2 = \tilde{\mathbf{F}}_{N_2}^H \mathbf{R}_2 \mathbf{\Psi} \mathbf{D}_G \mathbf{Z}_2^H \mathbf{B}_2 \bar{\mathbf{c}}_1$ and $\mathbf{v}_2 = \tilde{\mathbf{F}}_{N_2}^H \mathbf{R}_2 \mathbf{\Psi} \mathbf{D}_G \mathbf{Z}_2^H \mathbf{B}_2 \mathbf{w}_2$ are interference from the first slice and noise after DFT operation, respectively.

The data for UE 2 can be written as a point-wise multiplication with the filter and channel frequency response. Then we can readily design the linear one-tap channel equalization algorithms based on (15) and (16) as:

$$\mathbf{W}_i = (\mathbf{H}_{eff,i} \mathbf{H}_{eff,i}^H + \nu \mathbf{E}_i)^{-1} \mathbf{H}_{eff,i}^H \qquad (17)$$

where $\mathbf{E}_i$ is the diagonal matrix with the diagonal element being the interference plus noise power on the subcarriers. When $i = 1$, $\mathbf{E}_1 = \text{diag}(\tilde{\mathbf{F}}_{N_1}^H \mathbf{R}_1 \mathbf{A}_1^H \mathbf{B}_1 \bar{\mathbf{A}}_{2,k} \mathbf{C}_2 \tilde{\mathbf{F}}_{N_2} \tilde{\mathbf{F}}_{N_2}^H \mathbf{C}_2^H \bar{\mathbf{A}}_{2,k}^H \mathbf{B}_1^H \mathbf{A}_1 \mathbf{R}_1^H \tilde{\mathbf{F}}_{N_1}) + \sigma_1^2 \mathbf{I}_{M_1}$. When $i = 2$, $\mathbf{E}_2 = \text{diag}(\tilde{\mathbf{F}}_{N_2}^H \mathbf{R}_2 \mathbf{\Psi} \mathbf{D}_G \mathbf{Z}_2^H \mathbf{B}_2 \bar{\mathbf{c}}_1 \bar{\mathbf{c}}_1^H \mathbf{B}_2^H \mathbf{Z}_2 \mathbf{D}_G^H \mathbf{\Psi}^H \mathbf{R}_2^H \tilde{\mathbf{F}}_{N_2}) + \sigma_2^2 \mathbf{I}_{M_2}$. $\nu = 0$ is for the zero forcing equalizer and $\nu = 1$ is for the minimum mean square error (MMSE) equalizer. Note that with proper filter design or at low SNR, the interference can be assumed to be zero, then we have the approximation

$\mathbf{E}_1 \approx \sigma_1^2 \mathbf{I}_{M_1}$ and $\mathbf{E}_2 \approx \sigma_2^2 \mathbf{I}_{M_2}$. In this case, no interference signal information is required for MMSE equalization.

IV. NUMERICAL RESULTS

In this section, we investigate the proposed DBDF model and performance for the multi-service PNS system in terms of the signal mean square error (MSE) and bit error rate (BER) for both slices. The OFDM system is also considered in the simulation as a benchmark. The first and the second UEs are allocated 20% and 5% of the full bandwidth. Each slice/service contains 20 subcarriers and the corresponding DFT size for the two slices are 100 and 400, respectively. Thus, we have the subcarrier spacing relationship between the two services $\Delta f_1 = 4\Delta f_2$. In addition, we assume the RF down sampling factor in UE 2 is 20, i.e., the sampling rate at the UE 2 is only $1/20$ of the one used in the UE 1 or base station. The CP length for the two UEs are 10 and 40, respectively. We consider the LTE extended typical urban (ETU) channel, unless otherwise specified. The modulation scheme is 16-QAM (quadrature amplitude modulation). In addition, we consider the MMSE based one-tap channel frequency domain equalizer. F-OFDM waveform with matched filter at the receiver is considered in the paper for all simulations with windowed Sinc filter and filter length being half the DFT size [21].

To investigate the interference in the DBDF system due to the baseband and RF numerology mismatches, Fig. 2 shows the symbol MSE after channel equalization versus the subcarrier index for both slices with different values of guardband ΔB_1. To clearly show the ISBI change, we consider the AWGN (Additive white Gaussian noise) channel and $E_b/N_0 = 50$ dB in this simulation. However, a multipath fading channel will the considered in the next simulation. It can be seen that the signal in both slices has smaller interference at the middle of the subband than at the edge. The reason is that the F-OFDM system generates more interference at the edge than in the middle [5]. In addition, the interference level reduces when the guard band increases in slice 2, especially at the edge subcarriers. On the other hand, the MSE does not change significantly in slice 1 when the guard band increases. In terms of the ISBI, the simulation results show that a couple of subcarriers as guard band is sufficient.

The BER performance for both UEs for different guard band B_G and E_b/N_0 is shown in Fig. 3. It can be seen that the two UEs in the DBDF system can co-exist with satisfactory BER performance even with relatively small guard band between them. However, smaller guard band tends to cause an error floor in high E_b/N_0 region. Consistent with the MSE simulation results, slice 2 is more sensitive to the guard band than slice 1. In addition, it can be seen that the OFDM system cannot work properly in the DBDF multi-service system since slice 2 is seriously affected by ISBI.

V. CONCLUSIONS

The work introduced in this paper establishes a framework for the physical layer network slicing in terms of the signal multiplexing and isolation. Four different configurations are
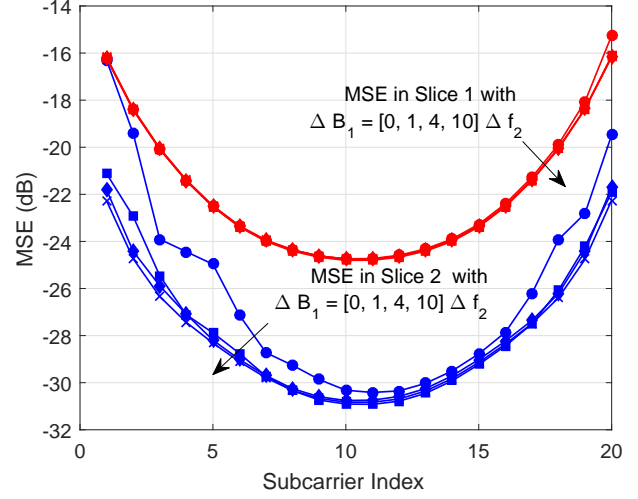

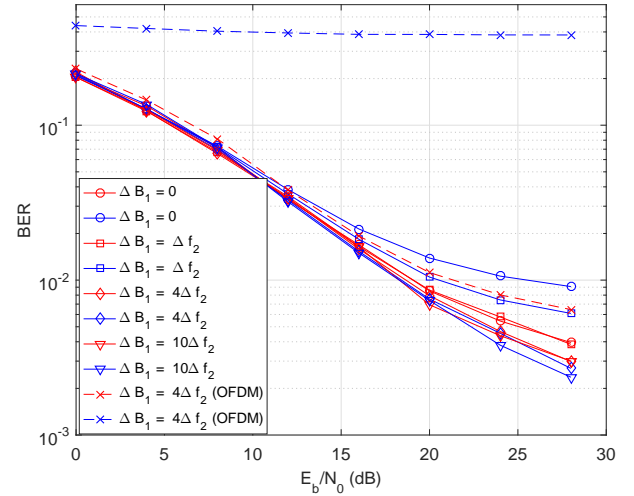Fig. 2. MSE versus subcarrier index with different guard band ΔB_1 (Red lines are for slice 1 and blue lines are for slice 2).

Fig. 3. BER versus E_b/N_o with different guard band ΔB_1 (Red lines are for slice 1 and blue lines are for slice 2).

defined and discussed for the PNS. By considering the most general case: slices with difference BB and different RF configuration (DBDR), the downlink system model for PNS is built based on the subband filtered multicarrier waveform. The desired signal and interference are derived separately for both slices. Simulation results show that a couple of subcarriers used as guard band between the two slices can efficiently reduce the interference caused by the BB and RF mismatch. The work presented in this paper provides a solution as to how the network slicing can be underpinned in the physical layer in a spectrum efficient way. The future work can be focused but not limited on the following aspects: 1), new channel equalization and estimation algorithms due to the slices configuration mismatch; 2), synchronization and random

access algorithms should be also proposed to support such new architecture in PNS; 3), Slice resource scheduling; 4), Extending to multi-input-multi-output (MIMO) case.

ACKNOWLEDGEMENT

REFERENCES

[1] M. Richart, J. Baliosian, J. Serrat, and J. L. Gorricho, "Resource slicing in virtual wireless networks: A survey," *IEEE Transactions on Network and Service Management*, vol. 13, no. 3, pp. 462–476, Sept 2016.

[2] C. Liang and F. R. Yu, "Wireless network virtualization: A survey, some research issues and challenges," *IEEE Communications Surveys Tutorials*, vol. 17, no. 1, pp. 358–380, Firstquarter 2015.

[3] Nokia, "Dynamic end-to-end network slicing for 5G," Tech. Rep., 2016.

[4] A. Ijaz, L. Zhang, M. Grau, A. Mohamed, S. Vural, A. U. Quddus, M. A. Imran, C. H. Foh, and R. Tafazolli, "Enabling Massive IoT in 5G and Beyond Systems: PHY Radio Frame Design Considerations," *IEEE Access*, vol. 4, pp. 3322–3339, 2016.

[5] L. Zhang, A. Ijaz, P. Xiao, A. Quddus, and R. Tafazolli, "Subband Filtered Multi-Carrier Systems for Multi-Service Wireless Communications," *IEEE Transactions on Wireless Communications*, vol. 16, no. 3, pp. 1893–1907, March 2017.

[6] L. Zhang, A. Ijaz, P. Xiao, and R. Tafazolli, "Multi-service System: An Enabler of Flexible 5G Air-Interface," *IEEE Communications Magazine*, pp. 1–9, 2017, to appear.

[7] 3GPP TR 36.802, "Narrowband Internet of Things (NB-IoT) – Technical Report for BS and UE radio transmission and reception (Release 13)," Tech. Rep., June 2016.

[8] Y. Wang, X. Lin, A. Adhikary, A. Grvlen, Y. Sui, J. B. Y.F. Blankenship, and H. Razaghi, "A Primer on 3GPP Narrowband Internet of Things (NB-IoT)," *[Online]. Available: https://arxiv.org/ftp/arxiv/papers/1606/1606.04171.pdf.*, 2016.

[9] X. Lin, A. Adhikary, and Y. P. E. Wang, "Random Access Preamble Design and Detection for 3GPP Narrowband IoT Systems," *IEEE Wireless Communications Letters*, vol. 5, no. 6, pp. 640–643, Dec 2016.

[10] C. Yu, L. Yu, Y. Wu, Y. He, and Q. Lu, "Uplink Scheduling and Link Adaptation for Narrowband Internet of Things Systems," *IEEE Access*, vol. PP, no. 99, pp. 1–1, 2017.

[11] L. Zhang, A. Ijaz, P. Xiao, and R. Tafazolli, "Channel equalization and interference analysis for uplink narrowband internet of things (nb-iot)," *IEEE Communications Letters*, vol. PP, no. 99, pp. 1–1, 2017.

[12] B. Farhang-Boroujeny, "OFDM versus filter bank multicarrier," *IEEE Signal Processing Magazine*, vol. 28, no. 3, pp. 92–112, May 2011.

[13] L. Zhang, P. Xiao, A. Zafar, A. ul Quddus, and R. Tafazolli, "FBMC system: An insight into doubly dispersive channel impact," *IEEE Transactions on Vehicular Technology*, vol. PP, no. 99, pp. 1–14, 2016.

[14] J. Du, P. Xiao, J. Wu, and Q. Chen, "Design of isotropic orthogonal transform algorithm-based multicarrier systems with blind channel estimation," *IET Communications*, vol. 6, pp. 2695–2704, November 2012.

[15] G. Fettweis, M. Krondorf, and S. Bittner, "GFDM - generalized frequency division multiplexing," in *IEEE Vehicular Technology Conference*, April 2009, pp. 1–4.

[16] N. Michailow, M. Matthe, I. Gaspar, A. Caldevilla, L. Mendes, A. Festag, and G. Fettweis, "Generalized frequency division multiplexing for 5th generation cellular networks," *IEEE Transactions on Communications*, vol. 62, no. 9, pp. 3045–3061, Sept 2014.

[17] L. Zhang, P. Xiao, and A. Quddus, "Cyclic prefix-based universal filtered multicarrier system and performance analysis," *IEEE Signal Processing Letters*, vol. 23, no. 9, pp. 1197–1201, Sept 2016.

[18] 5GNOW, "D3.2: 5G waveform candidate selection," Tech. Rep., 2014.

[19] Y. Chen, F. Schaich, and T. Wild, "Multiple access and waveforms for 5G: IDMA and universal filtered multi-carrier," in *IEEE Vehicular Technology Conference (VTC Spring)*, 2014, pp. 1–5.

[20] J. Abdoli, M. Jia, and J. Ma, "Filtered ofdm: A new waveform for future wireless systems," in *IEEE Signal Processing Advances in Wireless Communications (SPAWC)*, June 2015, pp. 66–70.

[21] X. Zhang, M. Jia, L. Chen, J. Ma, and J. Qiu, "Filtered-OFDM - enabler for flexible waveform in the 5th generation cellular networks," in *2015 IEEE Global Communications Conference*, Dec 2015, pp. 1–6.

[22] L. Zhang, A. Ijaz, P. Xiao, A. Quddus, and R. Tafazolli, "Single-rate and multi-rate multi-service systems for next generation and beyond communications," in *IEEE PIMRC*, Sept. 2016, pp. 1–6.